E×B flow velocity deduced from the poloidal motion of fluctuation patterns in neutral beam injected L-mode plasmas on KSTAR

W. Lee, J. Leem, G. S. Yun, H. K. Park, S. H. Ko, M. J. Choi, W. X. Wang, R. V. Budny, S. Ethier, Y. S. Park, N. C. Luhmann Jr., C. W. Domier, K. D. Lee, W. H. Ko, K. W. Kim, and KSTAR Team

Citation: Physics of Plasmas **23**, 052510 (2016); doi: 10.1063/1.4949350
View online: http://dx.doi.org/10.1063/1.4949350
View Table of Contents: http://scitation.aip.org/content/aip/journal/pop/23/5?ver=pdfcov
Published by the AIP Publishing

$E \times B$ flow velocity deduced from the poloidal motion of fluctuation patterns in neutral beam injected L-mode plasmas on KSTAR

W. Lee,[1] J. Leem,[2] G. S. Yun,[2] H. K. Park,[1] S. H. Ko,[3] M. J. Choi,[3] W. X. Wang,[4] R. V. Budny,[4] S. Ethier,[4] Y. S. Park,[5] N. C. Luhmann, Jr.,[6] C. W. Domier,[6] K. D. Lee,[3] W. H. Ko,[3] K. W. Kim,[7] and KSTAR Team
[1]*Ulsan National Institute of Science and Technology, Ulsan 44919, South Korea*
[2]*Pohang University of Science and Technology, Pohang, Gyeongbuk 37673, South Korea*
[3]*National Fusion Research Institute, Daejeon 34133, South Korea*
[4]*Princeton Plasma Physics Laboratory, Princeton, New Jersey 08543, USA*
[5]*Columbia University, New York, New York 10027, USA*
[6]*University of California at Davis, Davis, California 95616, USA*
[7]*Kyungpook National University, Daegu 41566, South Korea*

(Received 12 February 2016; accepted 15 April 2016; published online 12 May 2016)

A method for direct assessment of the equilibrium $E \times B$ flow velocity ($E \times B$ flow shear is responsible for the turbulence suppression and transport reduction in tokamak plasmas) is investigated based on two facts. The first one is that the apparent poloidal rotation speed of density fluctuation patterns is close to the turbulence rotation speed in the direction perpendicular to the local magnetic field line within the flux surface. And the second "well-known" fact is that the turbulence rotation velocity consists of the equilibrium $E \times B$ flow velocity and intrinsic phase velocity of turbulence in the $E \times B$ flow frame. In the core region of the low confinement (L-mode) discharges where a strong toroidal rotation is induced by neutral beam injection, the apparent poloidal velocities (and turbulence rotation velocities) are good approximations of the $E \times B$ flow velocities since linear gyrokinetic simulations suggest that the intrinsic phase velocity of the dominant turbulence is significantly lower than the apparent poloidal velocity. In the neutral beam injected L-mode plasmas, temporal and spatial scales of the measured turbulence are studied by comparing with the local equilibrium parameters relevant to the ion-scale turbulence. *Published by AIP Publishing.* [http://dx.doi.org/10.1063/1.4949350]

I. INTRODUCTION

In magnetically confined plasmas, heat and particle transport from the hot core to the cold edge is significantly enhanced by the turbulence. This issue has been critical in understanding the cross field energy transport. Therefore, the study of suppression mechanisms of the turbulence has been the prime research topic. One of the well-known mechanisms of turbulence suppression is an $E \times B$ flow shear, which was originally developed to explain the strong transport barrier formed at the edge of high confinement (H-mode) plasmas.[1] The sheared flow, which is induced by the spatially non-uniform radial electric field, can reduce the growth rate of the turbulence and breaks the radially elongated turbulent eddies, which are known as the path of heat and particle transport. Therefore, the measurements of $E \times B$ flow velocity (or radial electric field) and the corresponding radial gradient are important for understanding of the turbulence behavior.

$E \times B$ flow velocity or radial electric field in tokamaks has been obtained with several methods. The most widely used method is the simultaneous measurement of the toroidal and poloidal rotation velocities and density profile of impurity ions or main ions with toroidal and poloidal charge exchange recombination spectroscopy (CES) systems. With these parameters, the radial electric field can be determined from the radial force balance relationship[2–6]

$$E_r = U_\phi B_\theta - U_\theta B_\phi + \nabla P_i/(Zen_i), \quad (1)$$

where the toroidal velocity U_ϕ, the poloidal velocity U_θ, the pressure P_i, and the density n_i are the parameters of single species ions (impurity or main ions) with charge Ze, and B_ϕ and B_θ are the toroidal and poloidal magnetic fields. This method provides the radial electric field profile over a wide radial range so that one can evaluate the $E \times B$ flow shear. The second method is based on the measurement of the rotation velocity of density fluctuations in the direction perpendicular to the magnetic field with Doppler reflectometry,[7–9] and then, the intrinsic turbulence phase velocity estimated from simulations is subtracted from the measured rotation velocity. When the measured rotation velocity of fluctuation is sufficiently faster than the intrinsic turbulence phase velocity, it is close to the $E \times B$ flow velocity. The third method is a direct measurement of the electric field with multichannel motional Stark effect (MSE) polarimetry.[10]

In this paper, the equilibrium $E \times B$ flow velocity is deduced from the mean apparent poloidal rotation velocity of density fluctuation patterns, which are measured by a multichannel (poloidal 16 and radial 2) microwave imaging reflectometry (MIR) system.[11,12] This system measures ion-scale electron density fluctuations with poloidal wavenumber $k_\theta \lesssim 3\ \mathrm{cm}^{-1}$. This method is similar to the second method employing Doppler reflectometry, since the apparent poloidal velocity with MIR is close to the rotation velocity of fluctuations measured by Doppler reflectometry (this is precisely explained in Sec. II). This method can be applied with any diagnostics for 1D (in the poloidal direction) or 2D fluctuation

measurements such as beam emission spectroscopy (BES) and electron cyclotron emission imaging (ECEI). The $E \times B$ velocity measurement with MIR is useful in the Korea Superconducting Tokamak Advanced Research (KSTAR), since the poloidal CES system is only available in the outer region ($r/a > 0.6$) and the Doppler reflectometry is still being developed (to be installed in 2016 or 2017).

II. $E \times B$ FLOW VELOCITY DEDUCED FROM THE APPARENT POLOIDAL ROTATION OF FLUCTUATION PATTERNS

The rotation speed of the turbulence in the direction perpendicular to the local magnetic field line within the flux surface (simply "turbulence rotation velocity") can be decomposed into two parts

$$v_\perp = U_{E\times B} + \omega_0/k_\perp, \tag{2}$$

where $U_{E\times B}$ is the equilibrium $E \times B$ flow velocity, and $\omega_0/k_\perp$ is the intrinsic phase velocity of the turbulence in the $E \times B$ flow frame.[7–9,13–16] This equation originates from a spectral shift model ($\omega_\perp = k_\perp U_{E\times B} + \omega_0$) proposed to explain that the observed mode frequencies are consistent with the calculated ones when the spectral shifts due to the $E \times B$ rotation are included.[13–15] Although the equation was originally introduced to explain the discrepancy in the mode frequency (observed versus calculated), it has also been utilized to determine the $E \times B$ flow velocities from turbulence rotation measurements with Doppler reflectometry.[7–9,16] If the $E \times B$ flow velocity dominates, the measured turbulence rotation velocity can be a good approximation of the $E \times B$ flow velocity.[7,8,16]

Direct measurement of the intrinsic phase velocity is not trivial since the $E \times B$ flow velocity is nonzero in most plasmas. In addition, the intrinsic phase velocity can be comparable to or even smaller than the measurement error of the $E \times B$ flow velocity and thereby has been computed by numerical simulations. From linear gyrokinetic simulations under the condition of equilibrium $E_r = 0$, ω_0 is the real part of the dominant mode frequency corresponding to the wavenumber $k_\perp$, where the growth rate is maximum. It is known that the intrinsic phase velocity is predominantly small compared to the corresponding diamagnetic velocities,[9,15] i.e., smaller than the ion pressure diamagnetic velocity $U_{*i} = \nabla P_i/(Ze n_i B)$ for the ion temperature gradient (ITG) mode and the electron density diamagnetic velocity $U_{*e} = -T_e \nabla n_e/(e n_e B)$ for the trapped electron mode (TEM), where T_e and n_e are the electron temperature and density, respectively.

The turbulence rotation velocity can also be expressed as the sum of a different flow velocities and phase velocities in the new flow frame as

$$v_\perp = U_\perp + \omega/k_\perp, \tag{3}$$

where $U_\perp = -(U_\phi B_\theta - U_\theta B_\phi)/B$ is the plasma (or ion mass) flow velocity in the perpendicular direction. This equation is more intuitive than Eq. (2) since $U_\perp$ is the plasma flow velocity in the laboratory frame. Note that the plasma flow can be decomposed into the parallel and perpendicular components (with respect to the local magnetic field) or toroidal and poloidal components. From a different form of the radial force balance relation $U_\perp = U_{E\times B} + U_{*i}$ together with Eqs. (2) and (3), the phase velocity in the plasma flow frame is related to the intrinsic phase velocity as

$$\omega/k_\perp = -U_{*i} + \omega_0/k_\perp. \tag{4}$$

This relationship indicates that the phase velocity in the plasma flow frame is governed by the ion diamagnetic velocity since its magnitude is larger than that of the intrinsic phase velocity. Therefore, $\omega/k_\perp$ is generally in the electron diamagnetic direction regardless of the dominant turbulence. Note that the positive (negative) velocity indicates the rotation in the electron (ion) diamagnetic direction in this paper.

Turbulent structures are anisotropic and highly elongated along the magnetic field line ($\ell_\parallel \gg \ell_\perp$, where $\ell_\parallel$ and $\ell_\perp$ are the turbulence length scales parallel and perpendicular, respectively, to the magnetic field line within the flux surface). The poloidal velocity of the elongated turbulent structures measured by multichannel diagnostics (dubbed as "apparent poloidal velocity" in this paper) is given by[17,18]

$$v_\theta = -U_\phi \tan\alpha + U_\theta + \omega/k_\theta, \tag{5}$$

where α is the magnetic pitch angle, and $k_\theta = k_\perp \cos\alpha$ (see Fig. 1). The poloidal projection of the toroidal flow velocity $-U_\phi \tan\alpha$ is the dominant term in fast rotating plasmas by neutral beam injection (NBI); however, the three terms on the right-hand side can be comparable in slowly rotating plasmas. The meaning of the poloidal motion of turbulent structures measured by multichannel diagnostics is more precisely explained in Ref. 18. To determine the apparent poloidal velocity from time-dependent multichannel data, a time delayed cross correlation (TDCC) analysis is applied.[12,18] The apparent poloidal velocities are in the ion diamagnetic direction (clockwise) in the core region of neutral beam (NB) injected plasmas and often in the electron diamagnetic direction (counterclockwise) in the core of ohmic plasmas (probably due to the intrinsic toroidal rotation in the counterclockwise direction when viewed from above)[11] or the

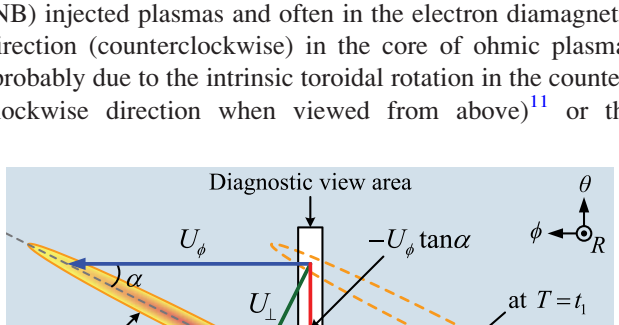

FIG. 1. Illustration representing the apparent poloidal motion (observed by a diagnostic) of a turbulent structure elongated along the magnetic field line. Here, it is assumed that $U_\theta = 0$ and $\omega/k_\theta = 0$. The poloidally projected toroidal flow velocity $-U_\phi \tan\alpha$ is the dominant term of the apparent poloidal velocity in NB injected plasmas. Note that the directions of the plasma current, the toroidal magnetic field, and the NBI are all clockwise in KSTAR when viewed from above.

pedestal of H-mode plasmas (probably due to the slow toroidal rotation in the edge region but large pressure gradient).[17] From Eqs. (4) and (5), it can be understood that the apparent poloidal velocity in the ion diamagnetic direction can be significantly reduced or reversed to the electron diamagnetic direction by the enhanced diamagnetic term in the steep ion pressure region (edge pedestal or internal transport barrier).

An important fact is that the apparent poloidal velocity is close to the turbulence rotation velocity as $v_\perp = v_\theta \cos\alpha$ from Eqs. (3) and (5). Based on this fact together with Eq. (2), multichannel imaging diagnostics such as MIR, BES, and ECEI can be utilized to measure the $E \times B$ flow velocity and corresponding radial electric field through the relationship

$$U_{E\times B} = v_\theta \cos\alpha - \omega_0/k_\perp. \tag{6}$$

If the intrinsic phase velocity is sufficiently smaller than the apparent poloidal velocity, the $E \times B$ flow velocity can be directly determined from the measured apparent poloidal velocity. A good agreement of this relationship was reported from a DIII-D experiment, where the apparent poloidal velocities measured by BES were similar to the $E \times B$ flow velocities obtained by the radial force balance.[19]

III. EXPERIMENTAL RESULTS

A. Equilibrium $E \times B$ flow velocities in NB injected L-mode discharges

In order to estimate the equilibrium $E \times B$ flow velocities, four NB injected low confinement (L-mode) discharges are analyzed. The basic operation parameters are as follows: the toroidal magnetic field on axis is 3.0 T (3.3 T for one discharge); the plasma current is 600 kA (700 kA for one discharge); and 1.43 MW NB using "source 1" was injected to the co-current direction for strong toroidal rotation for all discharges (0.7 MW electron cyclotron resonance heating (ECH) was additionally applied to one discharge). Figure 2 shows the radial profiles of the electron and ion temperatures, the electron density, the toroidal rotation speed, the safety factor, and the magnetic pitch angle. The electron temperature was measured by an electron cyclotron emission (ECE) radiometer, and the carbon ion (C^{6+}) temperature and the toroidal rotation velocity were measured by CES. Note that the electron temperature measurement was available only in the region of $R > 2.04$ m for the 3.3 T plasma due to the limited frequency range of the detection system, and a reasonable electron density profile was assumed for the L-mode discharges and normalized to the measured line average density. The safety factor and the magnetic pitch angle were deduced from the equilibrium reconstruction calculation with the EFIT code.[20]

The mean apparent poloidal velocities measured at $R \approx 2.0$–2.15 m (or $r/a \approx 0.4$–0.7) are 4–9 km/s in the ion diamagnetic direction (clockwise). Note that the cross correlation analysis is applied to 40 ms duration signals (amplitudes of complex signals) recorded at 1 MHz sampling rate and high-pass filtered at 100 kHz. Unavailability of the electron density profile measurement gives uncertainty in the MIR measurement position (assumed ± 5 cm), and this is the

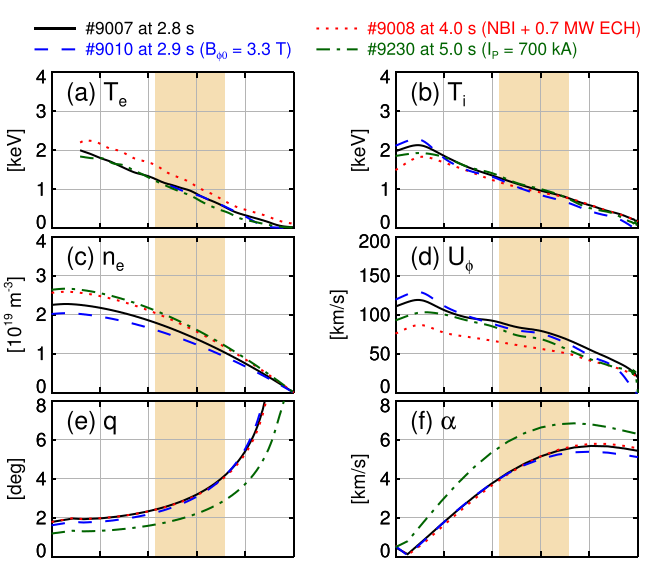

FIG. 2. Radial profiles of parameters of four NB injected L-mode discharges: (a) electron and (b) ion temperatures; (c) electron density; (d) toroidal flow velocity; (e) safety factor; and (f) magnetic pitch angle. The basic operation parameters are $B_{\phi 0} = 3.0$ T, $I_p = 600$ kA, and $P_{NB} = 1.43$ MW. The MIR measurement region is colored orange.

major error source ($\sim$10%) in the apparent poloidal velocity measurement. Note that the total error is $\sim$25% including the error of linear fitting ($\sim$5%) when applying the TDCC analysis and error in the optical system ($\sim$10%). Exact poloidal spans with 16 channels are obtained by ray tracing since the refraction effect near the cutoff layer cannot be neglected. Especially in the inner measurement ($r/a \sim 0.4$), the poloidal span is reduced by $\sim$11% with respect to the vacuum case. Since the magnetic pitch angle is less than 7°, $v_\perp \approx v_\theta$. The intrinsic phase velocities of the dominant turbulence from the linear gyrokinetic simulations with the GYRO code[21] are from -0.4 km/s to 0.2 km/s, as shown in Fig. 3(a), which are much slower than the measured apparent poloidal velocities and well within the measurement error of the apparent poloidal velocity. Accordingly, the measured apparent poloidal velocities are close to the $E \times B$ flow velocities. The equilibrium $E \times B$ flow velocity and the corresponding radial electric field $E_r = -U_{E\times B}B$ are shown in Figs. 3(b) and 3(c). For a discharge (shot #9010), the radial electric field profile is predicted from a neoclassical calculation with the TRANSP code[22] and represented by a blue dashed line in Fig. 3(c). The poloidal flow and ion pressure terms on the right hand side of Eq. (1) are calculated, since the measurement of the poloidal flow velocity and the ion pressure was not available for the discharges. The measured E_r is consistent with the neoclassical prediction.

The measured apparent poloidal velocities for shot #9010 are compared to those predicted from a turbulence simulation, including the toroidal flow effect by NBI with a nonlinear gyrokinetic code GTS.[23,24] Note that the TRANSP results such as the radial electric field were used for the initial condition of the GTS calculation. Figure 4(a) shows a time evolution of electron density fluctuations measured at $R \sim 215$ cm, and Fig. 4(b) shows a snapshot of 2D fluctuations simulated by GTS. The GTS result is taken from the

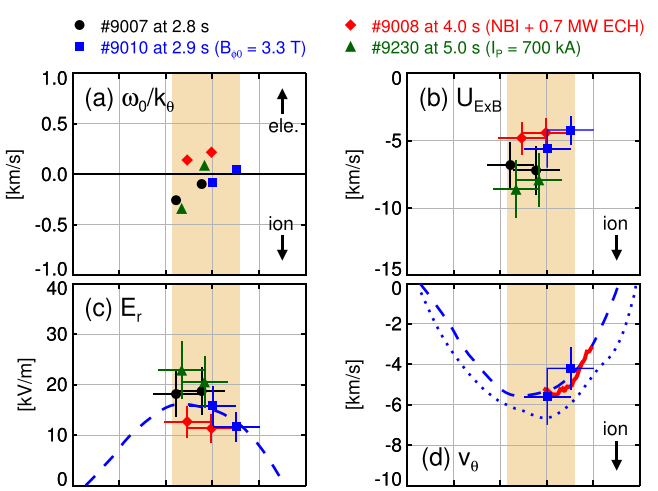

FIG. 3. Intrinsic phase velocities of dominant turbulence from the linear gyrokinetic simulations with GYRO, (b) measured v_θ which is close to $U_{E\times B}$, and (c) corresponding E_r (blue dashed line is the E_r profile calculated by TRANSP for shot #9010). (d) Measured v_θ (blue squares) for shot #9010 are compared to those from a nonlinear gyrokinetic simulation of turbulence with GTS (red solid line) and calculated $U_{E\times B}$ by TRANSP (dashed line). The dotted line indicates $-U_\phi \tan\alpha$.

saturated turbulence phase. Figures 4(c) and 4(d) illustrate the apparent poloidal velocities determined by the TDCC analysis. The measured value at $R \sim 215$ cm is smaller than the predicted value from the turbulence simulation, but the difference is within the measurement error bar. In Fig. 3(d), the measured values are compared to the predicted ones by GTS and TRANSP. Based on the GTS and TRANSP results, the turbulence contribution to the $E \times B$ velocity is in the ion diamagnetic direction.

B. Spatial and temporal scales of the measured turbulence

Spatial and temporal characteristic scales of the density turbulence in the NB injected L-mode discharges are estimated using the cross correlation analysis. The poloidal correlation length (ℓ_θ) of the density turbulence is determined by fitting a function $f(\Delta Z) = \cos(k_\theta \Delta Z)\exp(-|\Delta Z|/\ell_\theta)$ to the cross correlations with zero time lag, $C(\Delta Z \neq 0, \Delta t = 0)$.[25] Note that $\ell_\perp = \ell_\theta \cos\alpha \approx \ell_\theta$ since $\alpha < 7°$. Figure 5 shows an example of the cross correlation analysis. Since the turbulence is known to be driven by radial gradients of equilibrium temperature and density, the normalized poloidal correlation lengths ℓ_θ/ρ_i ($\rho_i = \sqrt{m_i T_i}/eB$ is the ion gyroradius) are compared with the normalized gradients R/L_*, where $L_* = \min(L_{T_i}, L_{n_e})$ and $L_X = X/|\partial X/\partial R|$ is the scale length of a parameter X. The result (from the small data set) does not show clear dependence on the radial gradient, as shown in Fig. 6(a).

A temporal scale of the turbulence, correlation time (τ_c) is estimated by fitting a function $f(\Delta t) = \exp[-|\Delta t_{\text{peak}}(\Delta Z)|/\tau_c]$ to the time lags of the peak cross correlations, as shown in Fig. 5(c). The correlation time is compared with four parameters: the ion drift time $\tau_* = \ell_\perp/U_{*i} \sim (\ell_\perp/\rho_i)L_*/v_{\text{th}i}$, where $v_{\text{th}i} = \sqrt{T_i/m_i}$ is the ion thermal speed;[25] the parallel ion streaming time $\tau_{\text{st}} = \ell_\parallel/v_{\text{th}i}$, where $\ell_\parallel \sim \pi q R$; the magnetic drift time $\tau_M = \ell_\perp/U_M \sim (\ell_\perp/\rho_i)R/v_{\text{th}i}$ (associated with ∇B and curvature drift); and the inverse $E \times B$ shearing rate $\tau_{E\times B} = 2\pi/\omega_{E\times B}$. Note that a simplified expression[26,27] of the Hahm-Burrell $E \times B$ shearing rate[28] is utilized based on the assumption of turbulence isotropy ($\ell_\perp \sim \ell_r$), and the E_r gradient of each discharge is evaluated with E_r values at two radial positions ($\Delta R \sim 5$ cm). Figures 6(c)–6(f) show linear dependence on the parameters especially on ion drift time and magnetic drift time. In a spherical tokamak, it was reported that the

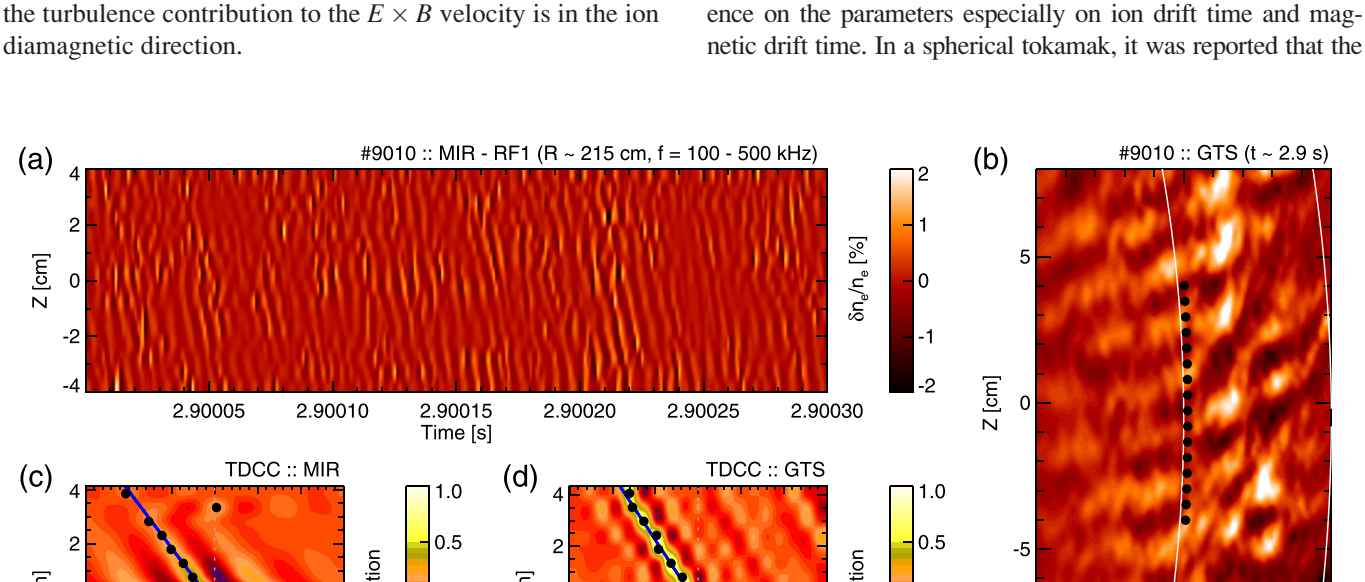

FIG. 4. Comparison between measurement and simulation for shot #9010 ($t \sim 2.9$ s): (a) time evolution of electron density fluctuations at $R \sim 215$ cm measured by MIR, (b) 2D electron density fluctuations (rotating clockwise) simulated by GTS (16 spots indicate the MIR measurement positions), and the mean apparent poloidal velocities of (c) the measured and (d) simulated fluctuations applying the time delayed cross correlation analysis.

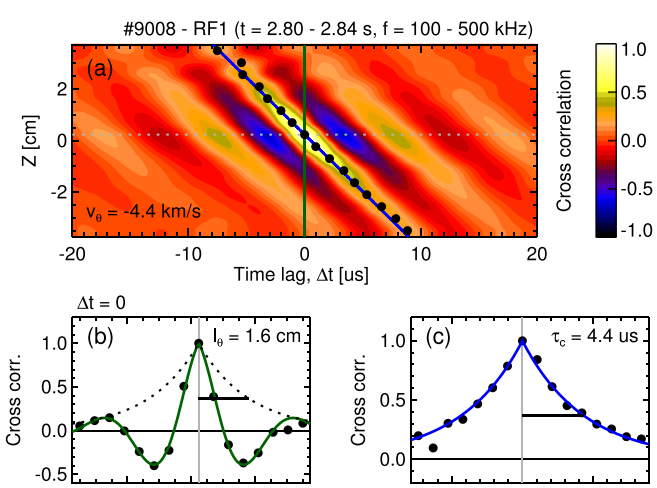

FIG. 5. (a) Cross correlations among poloidal channels and determined turbulence characteristics: (b) poloidal correlation length ℓ_θ and (c) correlation time τ_c.

correlation time of ion-scale turbulence is comparable with three parameters as $\tau_c \sim \tau_* \sim \tau_{st} \sim \tau_M$, and the measured turbulence was called critically balanced.[25,29] On the other hand, the correlation time in this experiment is about a third of the drift time and is much smaller than the streaming time and the magnetic drift time as $\tau_{st} \sim \tau_M \sim 17\,\tau_c$. Since $\tau_{st} \sim \tau_M$ as shown in Figs. 6(d) and 6(e), it is found that $\ell_\theta/\rho_i \sim \ell_\parallel/R \sim \pi q$, which is plotted in Fig. 6(b).

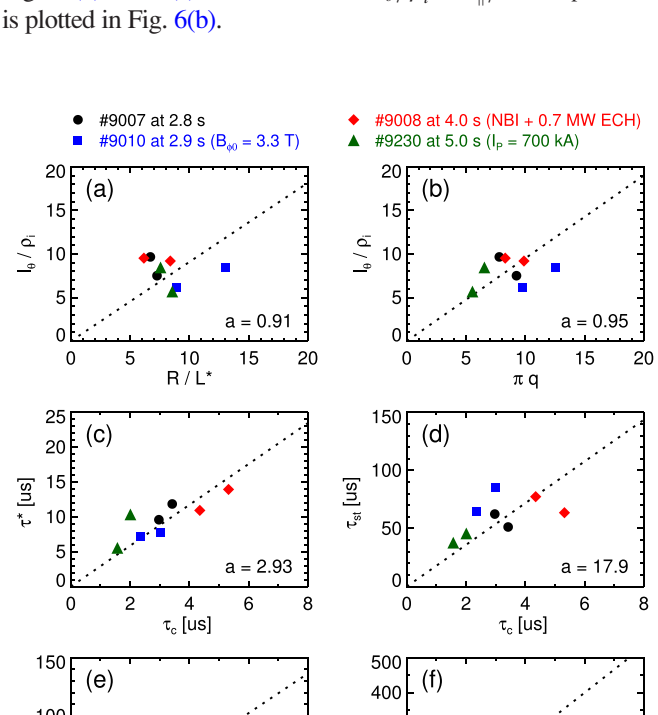

FIG. 6. Normalized poloidal correlation length versus (a) normalized gradient R/L_* and (b) safety factor. The relationship between the correlation time τ_c and four parameters: (c) ion drift time, (d) streaming time, (e) magnetic drift time, and (f) inverse $E \times B$ shearing rate.

IV. SUMMARY

The equilibrium $E \times B$ flow velocities are obtained by measuring the mean apparent poloidal velocity of the turbulent density fluctuation patterns with the MIR system in the core region of the NB injected L-mode discharges on KSTAR. The linear gyrokinetic simulations show that the intrinsic phase velocities of the dominant turbulence, which seem to be either the ITG mode or TEM, are sufficiently small compared to the apparent poloidal velocities. In this case, the apparent poloidal velocities are close to the $E \times B$ flow velocities.

The spatial and temporal characteristic scales of the measured turbulence in the NB injected L-mode discharges are estimated by utilizing a cross correlation analysis. The poloidal correlation length ($\ell_\theta/\rho_i = 5 - 10$) does not seem to be dependent on the gradients of ion temperature and density but on the safety factor. The correlation time ($\tau_c = 2$–$6\,\mu$s) shows the linear relationship with the local equilibrium parameters relevant to the ion-scale turbulence.

V. DISCUSSION

In this paper, only the L-mode plasmas are analyzed for the $E \times B$ flow velocity estimation since correlations among the poloidal channels in the H-mode plasmas are weak probably due to reduced turbulence, and weak correlations result in large fitting errors on the apparent poloidal velocity. This is a disadvantage of the method based on the cross correlations among multiple channels. In the H-mode, we need a different method to deduce more accurate apparent poloidal velocities. If there are long-lived coherent modes in the H-mode, exact apparent velocities can be easily determined as demonstrated in Ref. 17.

ACKNOWLEDGMENTS

We thank T. S. Hahm at Seoul National University and Y.-C. Ghim at Korea Advanced Institute of Science and Technology for valuable discussion on the poloidal velocity of the turbulent structure measured by MIR. This research was supported by the National R&D Program through the National Research Foundation of Korea (NRF) funded by the Ministry of Science, ICT and Future Planning (NRF-2014M1A7A1A03029865), and the U.S. DoE under Grant No. DE-FG02-99ER54531.

[1]K. H. Burrell, Phys. Plasmas **4**, 1499 (1997).
[2]K. Crombé, Y. Andrew, M. Brix, C. Giroud, S. Hacquin, N. C. Hawkes, A. Murari, M. F. F. Nave, J. Ongena, V. Parail, G. Van Oost, I. Voitsekhovitch, and K.-D. Zastrow, Phys. Rev. Lett. **95**, 155003 (2005).
[3]W. M. Solomon, K. H. Burrell, R. Andre, L. R. Baylor, R. Budny, P. Gohil, R. J. Groebner, G. T. Holocomb, W. A. Houlberg, and M. R. Wade, Phys. Plasmas **13**, 056116 (2006).
[4]T. Tala, Y. Andrew, K. Crombé, P. C. de Vries, X. Garbet, N. Hawkes, H. Nordman, K. Rantamäki, P. Strand, A. Thyagaraja, J. Weiland, Y. B. E. Asp, C. Challis, G. Corrigan, A. Eriksson, C. Giroud, M.-D. Hua, I. Jenkins, H. C. M. Knoops, X. Litaudon, P. Mantica, V. Naulin, V. Parail, K.-D. Zastrow, and JET-EFDA Contributors, Nucl. Fusion **47**, 1012 (2007).
[5]K. Crombé, Y. Andrew, T. M. Biewer, E. Blanco, P. C. de Vries, C. Giroud, N. C. Hawkes, A. Meigs, T. Tala, M. von Hellermann, K.-D. Zastrow, and JET EFDA Contributors, Plasma Phys. Controlled Fusion **51**, 055005 (2009).

[6]R. E. Bell, R. Andre, S. M. Kaye, R. A. Kolesnikov, B. P. LeBlanc, G. Rewoldt, W. X. Wang, and S. A. Sabbagh, Phys. Plasmas **17**, 082507 (2010).
[7]M. Hirsh, E. Holzhauer, J. Baldzuhn, B. Kurzan, and B. Scott, Plasma Phys. Controlled Fusion **43**, 1641 (2001).
[8]G. D. Conway, J. Schirmer, S. Klenge, W. Suttrop, E. Holzhauer, and ASDEX Upgrade Team, Plasma Phys. Controlled Fusion **46**, 951 (2004).
[9]G. D. Conway, C. Angioni, R. Dux, F. Ryter, A. G. Peeters, J. Schirmer, C. Troester, CFN Reflectometry Group, and ASDEX Upgrade Team, Nucl. Fusion **46**, S799 (2006).
[10]B. W. Rice, K. H. Burrell, L. L. Lao, and Y. R. Lin-Liu, Phys. Rev. Lett. **79**, 2694 (1997).
[11]W. Lee, J. Leem, G. S. Yun, H. K. Park, J. A. Lee, Y. B. Nam, Y. U. Nam, W. H. Ko, J. H. Jeong, Y. S. Bae, H. Park, K. W. Kim, C. W. Domier, and N. C. Luhmann, Jr., J. Instrum. **8**, C10018 (2013).
[12]W. Lee, J. Leem, J. A. Lee, Y. B. Nam, M. Kim, G. S. Yun, H. K. Park, Y. G. Kim, H. Park, K. W. Kim, C. W. Domier, N. C. Luhamnn, Jr., K. D. Lee, Y. U. Nam, W. H. Ko, J. H. Jeong, Y. S. Bae, and KSTAR Team, Nucl. Fusion **54**, 023012 (2014).
[13]R. A. Koch and W. M. Tang, Phys. Fluids **21**, 1236 (1978).
[14]C. X. Yu, D. L. Brower, S. J. Zhao, W. A. Peebles, N. C. Luhamnn, Jr., R. V. Bravence, J. Y. Chen, H. Lin, C. P. Ritz, P. M. Schoch, and X. Z. Yang, Phys. Fluids B **4**, 381 (1992).
[15]K. L. Wong, N. L. Bretz, T. S. Hahm, and E. Synakowski, Phys. Lett. A **236**, 339 (1997).
[16]J. C. Hillesheim, W. A. Peebles, T. L. Rhodes, L. Schmitz, T. A. Carter, P.-A. Gourdain, and G. Wang, Rev. Sci. Instrum. **80**, 083507 (2009).
[17]G. S. Yun, W. Lee, M. J. Choi, J. Lee, H. K. Park, C. W. Domier, N. C. Luhmann, Jr., B. Tobias, A. J. H. Donné, J. H. Lee, Y. M. Jeon, S. W. Yoon, and KSTAR Team, Phys. Plasmas **19**, 056114 (2012).
[18]Y.-c. Ghim, A. R. Field, D. Dunai, S. Zoletnik, L. Bardóczi, A. A. Schekochihin, and MAST Team, Plasma Phys. Controlled Fusion **54**, 095012 (2012).
[19]M. W. Shafer, R. J. Fonck, G. R. McKee, C. Holland, A. E. White, and D. J. Schlossberg, Phys. Plasmas **19**, 032504 (2012).
[20]L. L. Lao, H. St. John, R. D. Stambaugh, A. G. Kellman, and W. Pfeiffer, Nucl. Fusion **25**, 1611 (1985).
[21]J. Candy and R. E. Waltz, J. Comput. Phys. **186**, 545 (2003).
[22]R. V. Budny, Nucl. Fusion **42**, 1383 (2002).
[23]W. X. Wang, Z. Lin, W. M. Tang, W. W. Lee, S. Ethier, J. L. V. Lewandowski, G. Rewoldt, T. S. Hahm, and J. Manickam, Phys. Plasmas **13**, 092505 (2006).
[24]W. X. Wang, P. H. Diamond, T. S. Hahm, S. Ethier, G. Rewoldt, and W. M. Tang, Phys. Plasmas **17**, 072511 (2010).
[25]Y. C. Ghim, A. A. Schekochihin, A. R. Field, I. G. Abel, M. Barnes, G. Colyer, S. C. Cowley, F. I. Parra, D. Dunai, S. Zoletnik, and MAST Team, Phys. Rev. Lett. **110**, 145002 (2013).
[26]E. J. Synakowski, S. H. Batha, M. A. Beer, M. G. Bell, R. E. Bell, R. V. Budny, C. E. Bush, P. C. Efthimion, G. W. Hammett, T. S. Hahm, B. LeBlanc, F. Levinton, E. Mazzucato, H. Park, A. T. Ramsey, G. Rewoldt, S. D. Scott, G. Schmidt, W. M. Tang, G. Taylor, and M. C. Zarnstorff, Phys. Rev. Lett. **78**, 2972 (1997).
[27]P. Zhu, W. Horton, and H. Sugama, Phys. Plasmas **6**, 2503 (1999).
[28]T. S. Hahm and K. H. Burrell, Phys. Plasmas **2**, 1648 (1995).
[29]M. Barnes, F. I. Parra, and A. A. Schekochihin, Phys. Rev. Lett. **107**, 115003 (2011).